ELSEVIER

Composite Structures 62 (2003) 155–162

COMPOSITE STRUCTURES

www.elsevier.com/locate/compstruct

Modeling and vibration control of a plate coupled with piezoelectric material

Y.Y. Li *, L. Cheng, P. Li

Department of Mechanical Engineering, The Hong Kong Polytechnic University, Hung Hom, Kowloon, Hong Kong

Abstract

This paper investigates the design of μ-synthesis controller for vibration control of a plate with piezoelectric patches. A numerical model with the consideration of the coupling between the PZT actuators and host plate is first derived. Using the model, a μ-controller is synthesized, in which model uncertainties are quantified by uncertainty weights included in the control design process. Experiments are then performed to verify the effectiveness of the present design approach, using the dSPACE DS 1103 and simulation tools in conjunction with MATLAB/Simulink. It is shown that, as an alternative of purely experimental approach, the established model provides a useful tool for the controller design, pointing to a straightforward extension to the case of multi-layer composite laminates and other composite structures.

Keywords: Piezoelectric plate; Vibration control; Modeling; μ-synthesis; PZT actuation

1. Introduction

The use of composite plates, either fiber-reinforced or multi-layered, in various engineering situations has substantially increased over the past years owing to their high strength and stiffness. One of the most widely used structures is the laminated composite plate with piezoelectric materials, which has attracted the attention of many researchers in fields of structural vibration analysis, damage detection and vibration control, etc. [1–6]. Due to the intrinsic direct and converse effects of the piezoelectric materials, they can be used as sensors or actuators. Vibration control of smart piezoelectric composite plates has been a topic of a significant amount of investigations up to the present, and led to the development of many control strategies [5–8]. Piezoelectric material can either be piecewise over the structure surface [1] or occupying a whole layer [3]. In the latter case, the host plate and the piezoelectric layer form a composite multi-layer lamina.

Irrespective of the physical arrangement of the lamina, a crucial problem to be tackled during the controller design process is the robustness problem, which is caused by the discrepancy of modeling from the system identification error, disturbance (input) or high-frequency model truncation. To solve this problem, techniques such as the robust pole assignment, H_∞ control and μ-synthesis, etc. have been successfully developed and applied to suppress the vibration [9–12]. Among these approaches, μ-synthesis is an attractive method for the controller design because it allows the direct inclusion of system uncertainties in the design process, and provides a framework for analyzing the performance and stability of uncertain systems. Literature survey shows that although μ-synthesis has been successfully applied in vibration suppression of many flexible structures, such as manipulators or steering wheel, etc. [13–16], it has been seldom considered on the plate-like structures coupled with piezoelectric material. There is also a lack of experimental data.

It is known that μ-synthesis is a model-based control design technique requiring a detailed mathematical model of the structure including a characterization of system uncertainties. The system modeling is the first step of the design. An attempt was made in our recent work [17], in which a MIMO μ-controller was designed based on experimental approach. In order to avoid doing a large amount of laboratory works on experimental modeling, it would be interesting to seek possibilities of using numerical modeling for controller design.

* Corresponding author. Tel.: +852-2766-6669; fax: +852-2365-4703.

E-mail address: mmyylee@polyu.edu.hk (Y.Y. Li).

0263-8223/$ - see front matter © 2003 Elsevier Ltd. All rights reserved.
doi:10.1016/S0263-8223(03)00110-7

The possible involvement of the numerical modeling in the design process provides numerous possibilities in exploring different configurations and optimizing the sensor/actuator placement. This is even true when PZT actuators are used, since once they are glued on the structure surface, it is impossible to relocate them during experiments. This paper attempts to explore this avenue. It is pertinent to mention that this study does not try to find a novel control algorithm, which is always done by many controller experts. It will rather emphasis on the application of the μ-synthesis for vibration control of plate-like structures coupled with piezoelectric material, which will change the structural properties, such as natural frequencies and mode shapes (or nodal lines) to a large extend, and will subsequently affect the selection of weighting functions. Moreover, the framework established in this paper is very general. Although results presented use single-layer lamina with piece-wise PZTs, it can be easily extended to the case of multi-layer composite laminates.

This paper is organized as follows. The numerical model of the plate coupled with PZTs is first developed and described in state-space form in Section 2, and then validated by experiments. A μ-controller is then synthesized based on the simulated model, in which the model uncertainties are characterized and described by the weighting functions. Criteria on the selection of weighting functions are also presented. Section 3 elaborates the experimental setup, controller synthesis and result analysis. Two cases are tested to investigate the robustness of the designed controller. In Section 4 some conclusions are drawn.

2. Modeling and design of μ-controllers

2.1. Modeling

Consider a simply supported rectangular plate ($a \times b \times h$) with r pairs piezoceramic (PZT) bonded on both sides of the plate (see Fig. 1). Based on the Kirchhoff's assumption and the perfect bonding between the host plate and the PZT patches, the equation of motion for flexural motion of the structure under the action of an applied electric field and external disturbance $f(x,y,t)$ can be expressed by

$$\left(D_{11}\frac{\partial^4}{\partial x^4}+2(D_{12}+D_{66})\frac{\partial^4}{\partial x^2\,\partial y^2}+D_{22}\frac{\partial^4}{\partial y^4}\right)w(x,y,t)+\rho h\frac{\partial^2 w(x,y,t)}{\partial t^2}=f(x,y,t)+\sum_{\ell=1}^{r}D_\ell(x,y)V_\ell, \tag{1}$$

where $w(x,y,t)$ denotes the mid-plane transverse displacement of point (x,y) either on the plate or on the piezoelectric elements. D_{11}, D_{12}, D_{22} and D_{66} are the flexural rigidities of the plate in different directions,

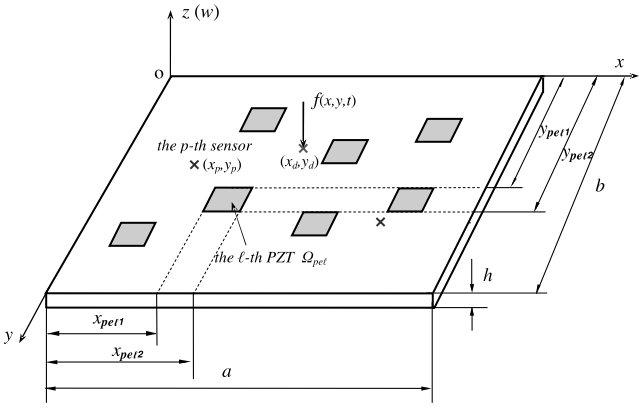

Fig. 1. Schematic diagram of a plate with piezoelectric patches.

$(E_{\mathrm{pl}}, \nu_{\mathrm{pl}})$ and $(E_{\mathrm{pe}}, \nu_{\mathrm{pe}})$ the Young's modulus and Poisson ratio of the plate and piezoelectric patch, respectively. $l_1=(h+h_{\mathrm{pe}})^3-h^3$, h_{pe} is the thickness of PZT and $\chi_{\mathrm{pe}_\ell}(x,y)$ the generalized location function described by the Heaviside function H as

$$\chi_{\mathrm{pe}_\ell}(x,y)=\lfloor H(x-x_{\mathrm{pe}_{\ell 1}})-H(x-x_{\mathrm{pe}_{\ell 2}})\rfloor \cdot \lfloor H(y-y_{\mathrm{pe}_{\ell 1}})-H(y-y_{\mathrm{pe}_{\ell 2}})\rfloor. \tag{2}$$

ρ is the mass per unit volume combining the properties of plate and PZT; V_ℓ the voltage applied to the ℓth pair of PZT patches (driven in anti-phase), and $D_\ell(x,y)=D_\ell\cdot\chi_{\mathrm{pe}_\ell}(x,y)$ the coefficient related to material properties of the ℓth PZT and its location. For an isotropic host plate with discretely distributed PZTs, Eq. (1) can be rewritten as

$$D\left(\frac{\partial^4}{\partial x^4}+2\frac{\partial^4}{\partial x^2\,\partial y^2}+\frac{\partial^4}{\partial y^4}\right)w(x,y,t)+\rho h\frac{\partial^2 w(x,y,t)}{\partial t^2}=f(x,y,t)+\sum_{\ell=1}^{r}D_\ell(x,y)V_\ell, \tag{1a}$$

where D is the equivalent flexible stiffness of the smart plate. In light of mode superposition theory, $w(x,y,t)$ can be formulated by

$$w(x,y,t)=\sum_{i=1}^{\infty}\sum_{j=1}^{\infty}\phi_{ij}(x,y)\eta_{ij}(t), \tag{3}$$

where $\eta_{ij}(t)$ and $\phi_{ij}(x,y)$ are the ijth modal coordinate and shape function, respectively. Substitution of Eq. (3) into Eq. (1a), pre-multiplication by $\phi_{kl}(x,y)$, integration over the whole plate, and with the considerations of structural damping and mode truncation gives a set of differential equations as

$$\ddot{\eta}_{kl}(t)+2\zeta_{kl}\omega_{kl}\dot{\eta}_{kl}(t)+\omega_{kl}^2\eta_{kl}(t)=\frac{1}{\rho hab}\left(f(t)\phi_{kl}(x_d,y_d)+\sum_{\ell=1}^{r}V_\ell D_\ell\cdot\int\!\!\int_{\Omega_{\mathrm{pe}_\ell}}\phi_{kl}(x,y)\,\mathrm{d}x\,\mathrm{d}y\right) \quad (k=1,\ldots,m;\ \ l=1,\ldots,n), \tag{4}$$

where ω_{kl} and ζ_{kl} are the klth natural frequency and damping ratio, respectively; (m,n) the numbers of modes after the truncation of the series. It is clear that the first term of right side of Eq. (4) is the disturbance force, and the second term the control force (V_ℓ the control inputs). Using the transformation $Q(t) = \{\eta^{\mathrm{T}}(t)\dot{\eta}^{\mathrm{T}}(t)\}^{\mathrm{T}}$, Eq. (4) is rewritten in the state-space form as

$$\dot{Q}(t) = \mathbf{A}Q(t) + \mathbf{B}u(t) + \mathbf{B}_f f(t), \tag{5}$$

where

$$\mathbf{A} = \begin{bmatrix} \mathbf{0} & \mathbf{I} \\ [-\omega_{kl}^2] & [-2\zeta_{kl}\omega_{kl}] \end{bmatrix}_{2mn\times 2mn}, \quad u = \begin{Bmatrix} V_1 \\ \vdots \\ V_r \end{Bmatrix}_{r\times 1},$$

$$\mathbf{B}_f = \frac{1}{\rho abh}\begin{bmatrix} 0 \\ \cdots \\ 0 \\ \phi_{11}(x_d, y_d) \\ \phi_{mn}(x_d, y_d) \end{bmatrix}_{2mn\times 1},$$

$$\mathbf{B} = \frac{1}{\rho abh}\begin{bmatrix} 0 & \cdots & 0 \\ .. & .. & .. \\ 0 & \cdots & 0 \\ D_1 \cdot \int\int_{\Omega_{\mathrm{pe}_1}} \phi_{11}(x,y)\,\mathrm{d}x\,\mathrm{d}y & .. & D_r \cdot \int\int_{\Omega_{\mathrm{pe}_r}} \phi_{11}(x,y)\,\mathrm{d}x\,\mathrm{d}y \\ .. & .. & .. \\ D_1 \cdot \int\int_{\Omega_{\mathrm{pe}_1}} \phi_{mn}(x,y)\,\mathrm{d}x\,\mathrm{d}y & .. & D_r \cdot \int\int_{\Omega_{\mathrm{pe}_r}} \phi_{mn}(x,y)\,\mathrm{d}x\,\mathrm{d}y \end{bmatrix}_{2mn\times r}. \tag{6}$$

Assuming that the outputs are a subset of charge signals measured by accelerometers, the charge output equations can be written as

$$y(t) = \mathbf{C}Q(t), \tag{7}$$

where

$$\mathbf{C} = \begin{bmatrix} \phi_{11}(x_{s_1}, y_{s_1}) & \cdots & \phi_{mn}(x_{s_1}, y_{s_1}) & 0 & .. & 0 \\ & .. & .. & .. & & \\ \phi_{11}(x_{s_p}, y_{s_p}) & \cdots & \phi_{mn}(x_{s_p}, y_{s_p}) & 0 & .. & 0 \end{bmatrix}_{p\times 2mn}. \tag{8}$$

The above development established the formalism, which will be used hereafter for controller design. However, structural mode shapes with PZT actuation can hardly be obtained analytically in most cases. To overcome this problem, a parallel formulation based on the variational principle is derived and the natural frequencies and modes shapes can be obtained numerically [18]. As a result, the aforementioned procedure can then be applied. As an alternative, the whole set of equation can be directly resolved to compute structural response under PZT actuation. It is pertinent to mention that the whole modeling approach is based on a very general variational approach requiring the calculating of the kinetic energy and potential energy of the system. Therefore the established approach can be easily extended to other types of composite structures. For different types of structures, only the way to calculate the potential energy differs.

The validity of the modeling is verified by comparing numerical and experimental results using an aluminum plate with dimensions of $0.38\times 0.3\times 0.003$ m. The plate is clamped on the left side, in which three pairs of bonded PZT patches (Sensortech BM500) are symmetrically adhered to the opposite sides of the structure (see Fig. 2(a)). The frequency response function (FRF) is used for comparison purposes. For the experimental testing, a pesudo-random signal was generated using a signal analyzer (B&K 3023), then amplified by a Piezo-Driver (Trek Model 603), and exerted on the PZTs at the center location of (0.135, 0.265). The response of the plate at point (0.155, 0.225) was measured using a B&K 4369 accelerometer. For the numerical modeling, the corresponding FRF is obtained from the state-space equation solved by Newmark method and FFT transformation. Fig. 2(b) shows the FRF curves obtained from the simulation and experimental test respectively. It can be observed that apart from the very low frequency region containing experimental noise, resonant peaks of these two curves coincide with each other, and tendencies of curves are basically the same. Obviously, the present model can simulate the real system well and is accurate enough for the controller synthesis.

2.2. μ-synthesis control

Eqs. (5) and (7) describe the dynamics of the structure, which can be denoted by the nominal system $G(s)$ in Laplace domain. In general, due to the identification error and unmodelled dynamics, the design of an active controller based on $G(s)$ might lead to poor or even unstable behavior of the closed-loop system. In such case, the uncertainties should be included in the model during the controller synthesis so as to achieve a certain degree of robustness and stability.

The block diagram of a μ-control system design is depicted in Fig. 3. In order to apply the general μ-synthesis framework, an interconnection structure is formed which consists of the model uncertainties and

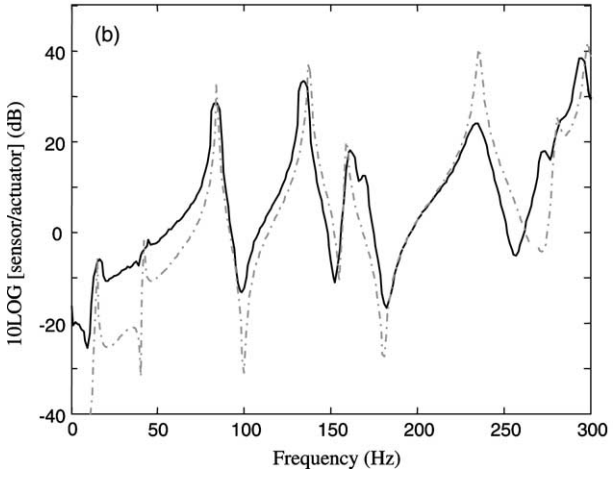

Fig. 2. (a) Experimental setup for modeling. (b) The frequency response function: (—) experimental result; (- - -) numerical result.

performance objectives, which are formulated in terms of weighting functions on system transfer functions. In this paper, the multiplicative uncertainty is assumed and $G(s)$ is modified by

$$\widetilde{G}(s) = (\mathbf{I} + \Delta G(s)) \cdot G(s), \tag{9}$$

where $G(s) = \mathbf{C}(s\mathbf{I} - \mathbf{A})^{-1}\mathbf{B}$, $\Delta G(s) = \Delta_G(s) \cdot W_G(s)$ with $\|\Delta_G(s)\|_\infty \leqslant 1$. Then, the augmented plant model $G_p(s)$ is described by the input–output scheme as

$$\begin{Bmatrix} z_1 \\ z_2 \\ z_\Delta \\ y \end{Bmatrix} = \left[\begin{array}{cc:c} 0 & 0 & W_1(s) \\ W_2(s) & W_2(s) & W_2(s)G(s) \\ \hdashline 0 & 0 & G(s) \cdot W_G(s) \\ \mathbf{I} & \mathbf{I} & G(s) \end{array}\right] \cdot \begin{Bmatrix} d \\ e_\Delta \\ u \end{Bmatrix} = G_P(s) \cdot \begin{Bmatrix} d \\ e_\Delta \\ u \end{Bmatrix}, \tag{10}$$

where z_1 and z_2 are a set of weighted exogenous outputs to be minimized, and $W_1(s)$ and $W_2(s)$ the weighting function matrices to be selected. For the design of μ-controllers, the objective is to find a stabilizing controller so that the weighted closed-loop transfer function is internally stable with

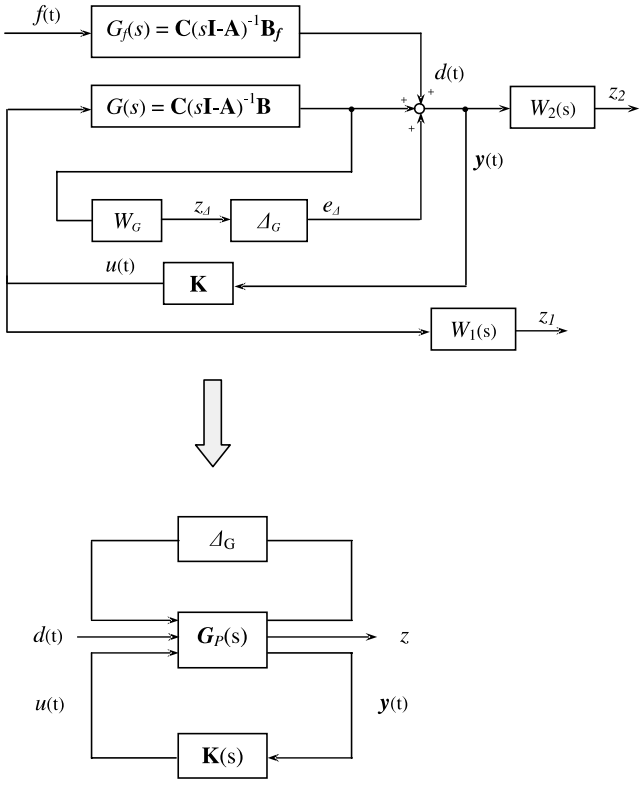

Fig. 3. Block diagram of a μ-synthesis control.

$$\left\| \begin{matrix} T_{z_1 d}(s) \\ T_{z_2 d}(s) \end{matrix} \right\|_\infty = \left\| \begin{matrix} W_1(s) \cdot K(s) \cdot [\mathbf{I} - (\mathbf{I} + \Delta_G(s)W_G(s))G(s)K(s)]^{-1} \\ W_2(s) \cdot [\mathbf{I} - (\mathbf{I} + \Delta_G(s)W_G(s))G(s)K(s)]^{-1} \end{matrix} \right\|_\infty \leqslant 1 \tag{11}$$

and

$$\sup_{\omega \in R} \mu_\Delta(G_P(\mathrm{j}\omega)) < 1, \tag{12}$$

where $\mu_\Delta(G_P)$ represents the structured singular value. Clearly, it is the standard μ-design, which can be solved using the "μ-analysis and synthesis" toolbox of MATLAB. The detailed description of the synthesis procedure can be found in Refs. [19–21].

During the controller synthesis, a vitally important issue to be addressed is the selection of weighting functions, which depend on the stability and performance required, the modes to be controlled and test conditions, etc. Some criteria are summarized as below.

2.2.1. Selection of $W_1(s)$

(1) When the high-frequency unmodelled dynamics is to be compensated for, $W_1(s)$ can be selected as a high-pass filter covering the higher vibration modes so as to control high-frequency roll-off, and the cutoff frequency

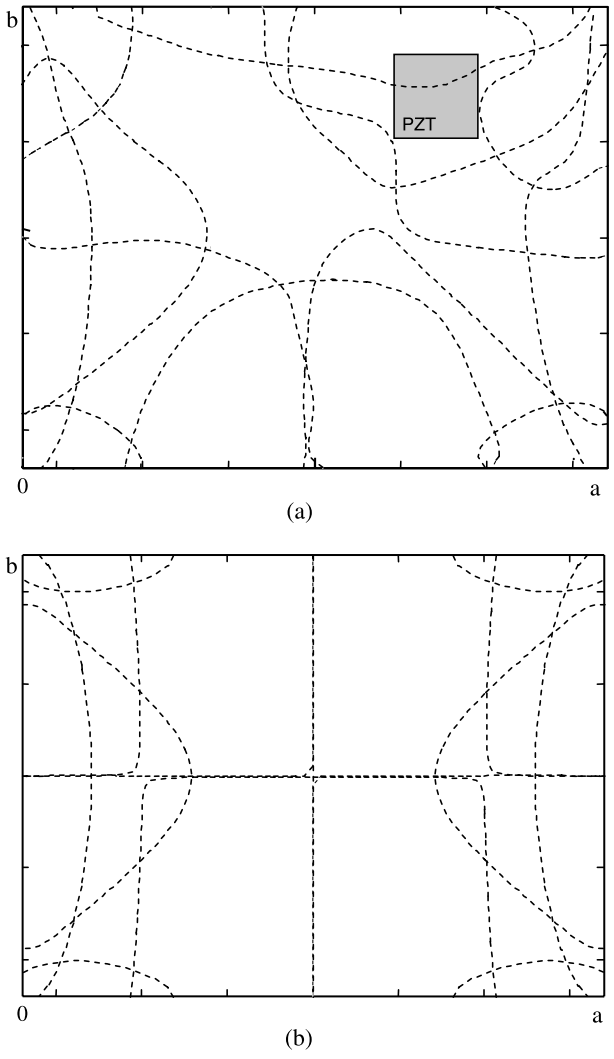

Fig. 4. Distribution of nodal lines of the *first five* strain modes (a) with PZT; (b) without PZT.

of $W_1(s)$ is set lower than the maximal frequency ω_{mn} of the designed model to avoid spillover problem. In this regard, the location of actuators plays a crucial role. In fact, it relates to the controllability analysis and the actuators are usually located at strain nodes of mode ω_{mn+1} to reduce system uncertainties. However, when the PZTs are used as actuators, the nodal lines will be changed due to the coupling between the PZTs and the host structure. An example is illustrated in Fig. 4, which shows the distributions of nodal lines for the *first five* strain modes of the structure with and without PZT actuation. It can be observed that the distribution of nodal lines with PZTs is highly irregular compared with their counterparts without PZTs. As a result, a coupled model, considering the electromechanical properties of the PZTs, is very important. This issue should also be considered when selecting $W_1(s)$.

(2) Under test conditions, $W_1(s)$ should be properly selected to prevent the saturation of controller output due to the limit of output voltage of hardware. For example, when the DS1103 D/A converter is used, $W_1(s)$ will be set as 0.1 to prevent the saturation due to the ± 10 V limits of converter output.

2.2.2. Selection of $W_2(s)$

The introduction of $W_2(s)$ is to reduce the influence of disturbance on outputs so as to improve robust performance. In general, in order to suppress low-frequency vibration, $W_2(s)$ can be set as a low-pass weighting filter with large amplitude, which is equivalent to adding damping to the system.

3. Experimental verification

3.1. Experimental setup

The experimental setup used for vibration control is schematically shown in Fig. 5. The test structure is the same as the one used in simulation described in Section 2 with partial clamping on the right side. During the test, one pair of PZTs (d_1) is used to generate the disturbance and two others (c_1 and c_2) to produce control forces. Firstly, the responses of the plate at locations s_1 and s_2 are monitored using two accelerometers (B&K 4369) and amplified using B&K 2635 charge amplifiers. Signals were then filtered by the Band-pass filters (YE-3790) and fed to a digital control system, which was built on a platform consisting of Matlab/Simulink software and a dSPACE DS 1103 controller in a computer. Control signals generated by the controller were amplified by a Piezo-Driver (Trek Model 700), and exerted on to the structure at c_1 and c_2 through PZTs, which are activated 180° out-of-phase. The sampling time is 0.25 ms (sampling frequency 4 kHz). A white noise generated from an FFT analyzer (B&K 3023) is taken as primary disturbance.

3.2. Controller synthesis and implementation

The *D–K* iteration is adopted to perform the synthesis procedure [20]. Since the weightings are included during the controller synthesis instead of the control system implementation, they should be determined in advance. For this case study, $W_1(s)$ was chosen as

$$W_1(s) = \begin{bmatrix} 0.1 & \\ & 0.1 \end{bmatrix}$$

to limit the maximal output for DS 1103 D/A converter, while the performance weighting $W_2(s)$ was selected based on the desired controller bandwidth and the frequency of the truncated vibration mode. The weighting for each control input can be modeled by the second-order transfer function as (see Fig. 6)

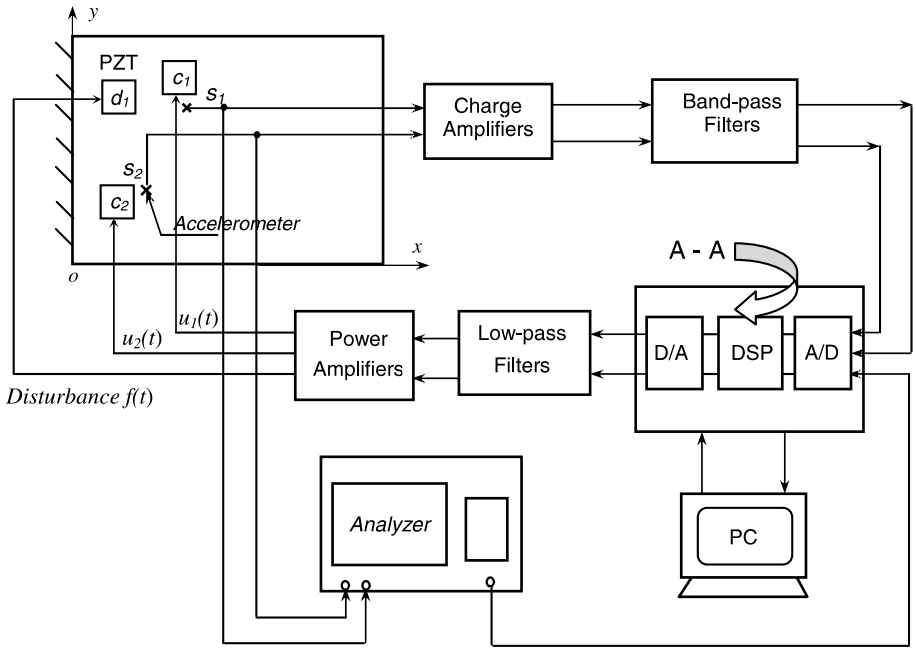

A – A: The Matlab/Simulink model for μ-control

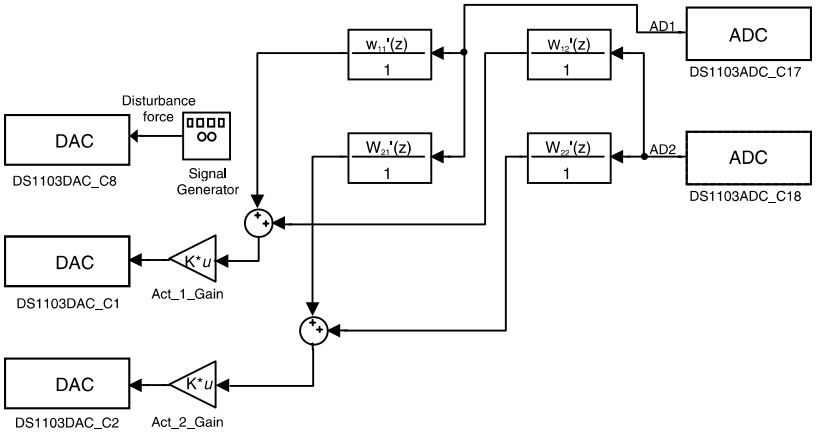

Fig. 5. Schematic diagram of the experimental setup.

$$W_2(s) = \mathrm{diag}(w_2(s)w_2(s)),$$
$$w_2(s) = \frac{3000s + 1}{2s^2 + 1720s + 911184}. \quad (13)$$

In addition, the multiplicative uncertainty weight $W_G(s)$ was selected to be

$$W_G(s) = \frac{3s + 100}{4s + 2000} \cdot \begin{bmatrix} 1 & \\ & 1 \end{bmatrix}. \quad (14)$$

In light of these weightings, a 22-order μ-controller was obtained after five iterations and model reduction, and implemented on the dSPACE DS 1103 control platform.

3.3. Experimental results

Two cases were tested to investigate the robustness of the designed controller. For the "nominal case" configuration, the modal parameters identified from the modeling was utilized to construct the plant $G(s)$; while for the "uncertain case", small masses were added to the structure to change modal frequencies so as to simulate model uncertainty. The same μ-controller was adopted and the control effect was evaluated from the curve of power spectrum.

Fig. 7(a) and (b) show the curves of power spectrum for the "nominal case" with and without μ-control at s_1 and s_2, respectively. It can be seen that peaks of the *first four* modes decrease after control. This reduction is

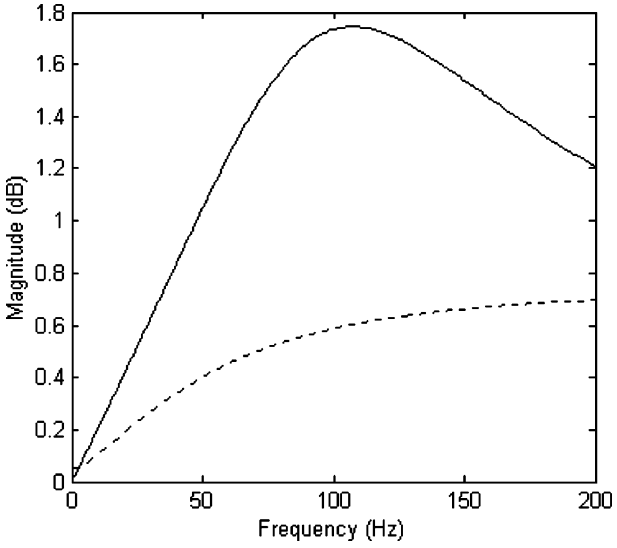

Fig. 6. The weighting functions of $W_2(s)$ (—) and $W_3(s)$ (- - -).

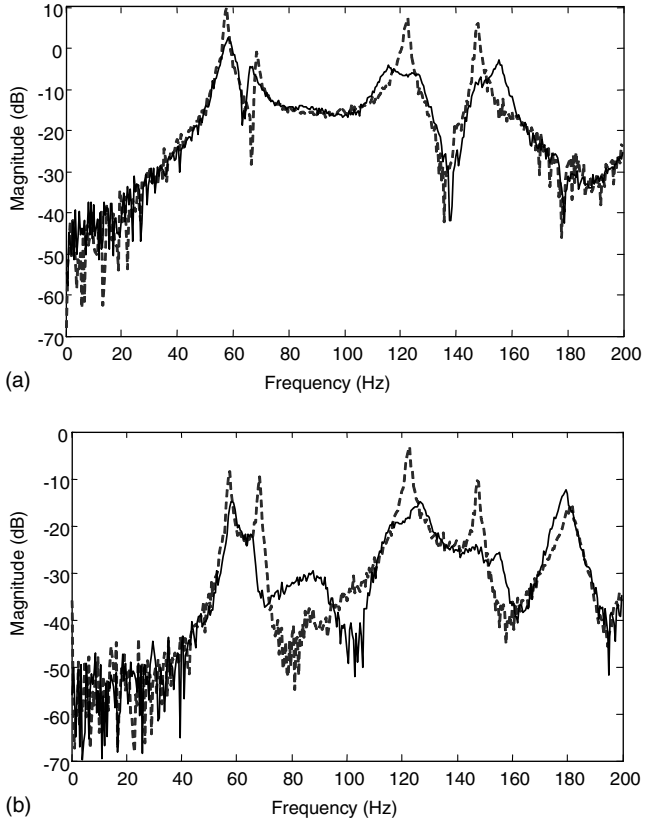

Fig. 7. The power spectrums of the sensor at (a) s_1 and (b) s_2 for the nominal case controller off (open loop): dashed; controller on (closed loop): solid line.

especially obvious for modes 2–4 in Fig. 7(b), in which a maximum attenuation of approximate 20 dB is obtained in terms of vibration magnitude, due to a significant amount of damping added to these modes. It is noticed however, that a little spillover occurs for mode 5. One plausible reason is that the natural frequency of mode 5

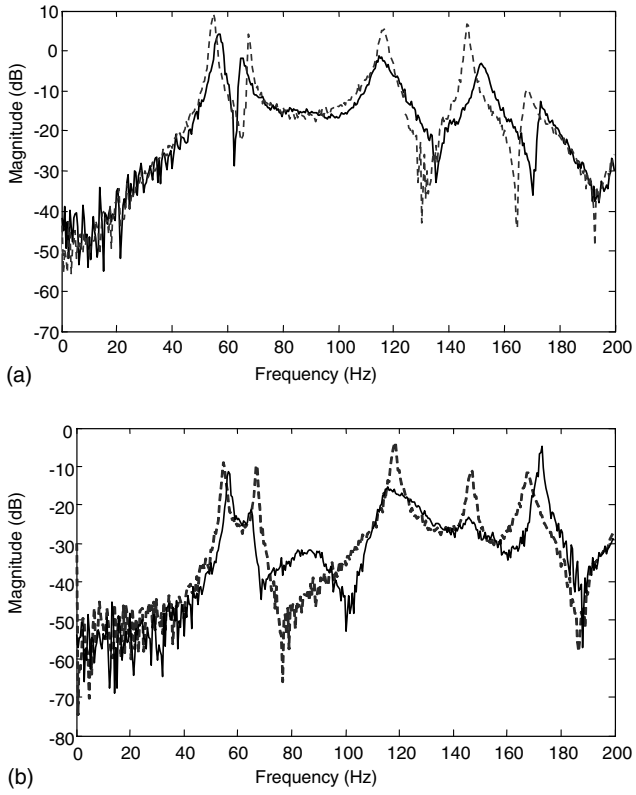

Fig. 8. The power spectrums of the sensor at (a) s_1 and (b) s_2 for the uncertain case controller off: (- - -); controller on: (—).

(180 Hz) is closed to the truncated frequency (200 Hz), which can affect the control performance at this region. The result can be improved by extending the truncated frequency and assigning the PZT at the nodal lines of mode 6.

In order to investigate the robustness of the designed controller against the parameter variations, three masses (m_1 with weight 10 g at location (0.29, 0.09), m_2 and m_3 with weight 21 g at locations (0.205, 0.15) and (0.12, 0.18), respectively) were added to the plate so as to change natural frequencies of the structure. Tests were carried out using the same controller. Fig. 8(a) and (b) show the curves of power spectra of the "uncertain case" with and without μ-control at s_1 and s_2, respectively. Similar to the result obtained for the "nominal case", the *first four* vibration modes are well suppressed. The addition of the masses does not seem to reduce the control efficiency of the controller. Similar tests using other configuration also confirm the observation made above. The μ-controller designed using the present approach is rather robust in handling parameter variations.

4. Conclusions

The application of μ-synthesis for vibration control of plate-like structures with PZT actuation is investigated.

Since μ-synthesis is a model-based control, numerical modeling of the coupled structure is developed and validated by experiments, showing a satisfactory agreement between both. Based on the numerical model, a MIMO μ-controller is synthesized and the selection of weightings is discussed. Two cases of experiment tests are carried out. The "nominal case" is used to validate the effectiveness of the designed μ-controller for vibration suppression, while the "uncertain case" to investigate its robustness. It is demonstrated that the established model can provide all information needed for the controller design and be further used in experiments. Experimental results also show that the μ-controller designed using the present scheme can provide robust stability and performance for vibration suppression of plates with model uncertainties.

As a final note, it is pertinent to mention that although a single-layer lamina with piece-wise PZTs was used for discussion, the general procedure for controller design applies to the multi-layer laminates with PZTs covering the whole surface. When fibre-reinforced composite material is involved, the variational approach can also handle the modeling problem using the framework established in this paper to achieve the final goal for controller design.

Acknowledgements

The authors would like to thank the Research Committee of the Hong Kong Polytechnic University and the Research Grants Council of Hong Kong Special Administrative Region, China for the financial support to this project (Grant no. PolyU 5165/02E).

References

[1] Lee CK. Theory of laminated piezoelectric plates for the design of distributed sensors/actuators. Part I. Governing equations and reciprocal relationships. J Acoust Soc Am 1990;87(3):1144–58.
[2] Heyliger P, Saravanos DA. Exact free-vibration analysis of laminated plates with embedded piezoelectric layers. J Acoust Soc Am 1995;98(3):1547–57.
[3] Gopinathan SV, Varadan VV, Varadan VK. A review and critique of theories for piezoelectric laminates. Smart Mater Struct 2000;9(1):24–48.
[4] Jian XH, Tzou HS, Lissenden CJ, Penn LS. Damage detection by piezoelectric patches in a free vibration method. J Compos Mater 1997;31(4):345–59.
[5] Hwang WS, Hwang W, Park HC. Vibration control of laminated composite plate with piezoelectric sensor actuator—active and passive control methods. Mech Syst Signal Process 1994;8(5):571–83.
[6] Lin CC, Huang HN. Vibration control of beam-plates with bonded piezoelectric sensors and actuators. Comput Struct 1999;73(1–5):239–48.
[7] Han JH, Rew KH, Lee I. An experimental study of active vibration control of composite structures with a piezo-ceramic actuator and a piezo-film sensor. Smart Mater Struct 1997;6(5):549–58.
[8] Jha R, Rower J. Experimental investigation of active vibration control using neural networks and piezoelectric actuators. Smart Mater Struct 2002;11(1):115–21.
[9] Sadri AM, Wynne RJ, Wright JR. Robust strategies for active vibration control of plate-like structures: theory and experiment. In: Proceedings of the Institution of Mechanical Engineers Part I. J Syst Control Eng 1999;213(16):489–504.
[10] Hwang JK, Choi CH, Song CK, Lee JM. Robust LQG control of an all-clamped thin plate with piezoelectric actuators/sensors. IEEE/ASME Trans Mechatron 1997;2(3):205–12.
[11] Kar IN, Miyakura T, Seto K. Bending and torsional vibration control of a flexible plate structure using H_∞-based robust control law. IEEE Trans Control Syst Technol 2000;8(3):545–53.
[12] Li YY, Yam LH. Robust control of vibrating thin plates by mean of variable parameter feedback and model-based fuzzy strategies. Comput Struct 2001;79(11):1109–19.
[13] Nonami K, Nishimura H, Tian HQ. H_∞/μ control-based frequency-shaped sliding mode control for flexible structures. JSME Int J Ser C—Dynam Control Robot Des Manufact 1996;39(3):493–501.
[14] Karkoub M, Balas G, Tamma K, Donath M. Robust control of flexible manipulators via μ-synthesis. Control Eng Practice 2000;8(7):725–34.
[15] Zhu Y, Qiu JH, Tani J, Suzuki S, Urushiyama Y, Hontani Y. Vibration control of a steering wheel using piezoelectric actuators. J Intelligent Mater Syst Struct 1999;10(2):92–9.
[16] Bai MR, Liu W. Control design of active vibration isolation using μ-synthesis. J Sound Vib 2002;257(1):157–75.
[17] Li P, Cheng L, Li YY, Chen N. Robust control of a vibrating plate using μ-synthesis approach. Thin-Walled Structures, in press, 2003.
[18] Proulx B, Cheng L. Dynamic analysis of piezoceramic actuation effects on plate vibrations. Thin-Walled Struct 2000;37(2):147–62.
[19] Active Control Experts, Inc., Smart ID System Identification Software, Cambridge, MA, 1995.
[20] Balas G, Doyle J, Glover K, Packard A, Smith R. μ-analysis and synthesis toolbox, MUSYN Inc. and MATHWORKS Inc., Minneapolis, MN, 1995.
[21] Zhou K, Doyle J, Glover K. Robust and optimal control. Englewood Cliffs, NJ: Prentice-Hall; 1996.